

# **Analysis of a new concept in spline design for transmission output shafts**

Kin S. Yeung

*Ford Motor Company, Dearborn, MI, 24121, USA.*

*Email: kyeung@ford.com*

## **Abstract**

The performance of an output shaft can be improved by adding a taper in the axial direction to its external spline. The optimal taper depends on the design torque and the stress criterion. The largest maximum principal stress in the shaft can be reduced by as much as 15% if the spline is tapered  $0.54^\circ$ . This type of reduction in stress would typically result in greater than a factor of two improvement in fatigue life. Conversely, it can be viewed as increasing the maximum spline fatigue load by 15%.

## **Introduction**

A spline is a geometric feature used to join one shaft to another. It transmits torsion, but permits axial sliding.

The current practice for designing splines to carry a torque is to use involute splines with no helix angle or taper on the external tooth. The size of the spline, the number of teeth and the engaged length of splines are chosen to satisfy size and performance constraints. In preliminary design, all teeth of the spline are assumed to carry an equal amount of load. Stress calculations are primarily based on experience and simple strength of material formulas [1,2]. Our current design practice also assumes that the load distribution does not change with respect to the distance along the axial direction of splines (the direction of the engaged length). Based on intuition, the load along the axial direction is not evenly distributed, especially on splines with long effective engaged length. It has long been surmised that the performance of the spline and shaft could be improved if a taper were added to help distribute the load on the spline. A literature survey reveals no data, either experimentally or analytically, exists to prove or disprove this conjecture.

The first objective of this project is to determine if adding a taper in the axial direction of a shaft to the external spline teeth on an output shaft is beneficial in reducing the spline stresses and therefore increasing the performance of the shaft. The second objective is to determine the optimum amount of taper if taper is beneficial.

## **Boundary Element Method**

The BEASY code [3] was used to perform the stress analyses. BEASY is based on the boundary element method (BEM). Since BEM is not as popular as the finite element method (FEM) in the automobile industry, a brief discussion of this method is in the following.

The fundamental governing equation for FEM [4] and BEM [5] involves both surface and volume integrals. Within the context of FEM, the volume integral is discretized into finite elements. In BEM, the volume integrals are analytically transformed to surface integrals. The resulting equation in BEM consists of only surface integrals. The surface integrals are then subdivided into elements. Thus removal of the volume integrals in BEM leads to a boundary-only description model.

A successful removal of the volume integral depends on availability of known solutions, called fundamental solutions [5]. These solutions describe the displacement and traction fields at the field point in infinite materials, usually linear elastic, as a result of an applied load at the source point in terms of a Dirac delta function. The Dirac delta function corresponds loosely to a unit point load. Consequently BEM can only handle those problems where fundamental solutions exist. The advantages and disadvantages of BEM as compared to FEM can be found from [7].

## **BEASY Contact Assumptions**

Under a torsional load, some surfaces of the external and internal splines may come into contact with each other while others may separate. Contact modeling is an important aspect for a successful stress analysis of splines.

The use of BEM to analyze contact problems has been documented in [5]. Since contact is a nonlinear problem, an iterative scheme is required. In this scheme, the loads applied in the analysis are incrementally increased and the effect on the contact area is considered. To start the first load step, an initial guess is made for the configuration of the contact surfaces, i.e. which parts have separated and which parts are in contact. The analysis is carried out and the resulting contact

mode is compared to the initial guess. If they do not match, i.e. the solution has not converged, the initial contact mode is modified and a further analysis or iteration is performed until convergence, within user defined or default tolerances, is obtained. BEASY uses the number of DOF that has converged on the contact surfaces in the analysis as tolerances to decide if a solution is acceptable or not. The next load step is then applied and the process repeated until convergence is achieved for the final load step.

There are two popular methods to find a contact solution: the penalty method and the constraint equation method. The BEASY code uses the constraint equation method [3]. In this method, constraint equations are enforced in both the tangential and normal directions in terms of tractions with and without friction, and displacements on potential contact/separation surfaces.

There are two types of contact: an external and an internal contact. An external contact models the effect of a deformable body coming into contact with some external rigid surface. Internal contact simulates the effects of initial gaps between different deformable components or zones in the same model. To model contact in BEASY it is not necessary for the users to generate master and slave contact surfaces separated by initial gaps.

In an external contact problem, BEASY only requires the users to predefine the likely contact area in the model, where the initial gaps are applied as boundary conditions.

For an internal contact problem, the two bodies or components coming into contact are modeled as separate zones and the likely contact area is modeled as an interface between the them. The initial gaps are applied over the interface as boundary conditions. Elements are then created on the surfaces including the interface. BEASY automatically generates a set of elements along the contact area, one set of elements belonging to each of the zones. The elements are no longer treated as interface elements but as boundary elements to their particular zone.

For non-zero gaps, the formulation in BEASY is an approximation to the physical situation. According to the formulation, BEASY only uses the initial gaps to monitor the relative movement of the bodies. These initial gaps are not used to calculate the actual dimensions of the bodies. This assumption is appropriate for small initial gaps. As in all small displacement formulation, the change of stiffness of the components as a result of contact is assumed to be negligible. The assumption is valid as long as the applied load is small.

## Spline Profile

The most widely used spline profile for parallel axis gears is the involute. One method by which an involute profile can be generated is by tracing a point on a string as it is unwound from a circle. The circle represents the base circle. The corresponding diameter is the base diameter. The string always remains tangent to the base circle as it is unwound from the base circle, and the string is always perpendicular to the surface of the involute curve.

A spline can be one of two types, internal and external splines. Splines are used in pairs with an internal spline on one component and an external spline on the other component. The splines have teeth located in a circular direction. An internal spline has teeth protruding inward in a radial direction of the base circle. External spline teeth protrude outward in a radial direction of the base circle. The engaged length represents the distance measured in the axial direction of the amount of spline in contact.

The spline for this project belongs to the involute type. Figure 1 shows a typical tooth cross-section of the external and internal splines.

## Boundary Element Model

There are two components in this model: a shaft with an external spline and a side gear with an internal spline. Since the deformation of each tooth is the same, a cyclic-symmetrical boundary condition is imposed to reduce the size of the physical model to the one shown in Figure 2. On the surface at  $z = 53$  mm, a torsion shear is applied and the displacement is constrained in the axial ( $z$ ) direction. All three DOF are constrained on the exterior surface of the side gear. For considering contact, each component is modeled as a different zone. There are 655 elements in the entire model, primarily Q3 (quadrilateral elements with nine nodes) and some T3 (triangular elements with six nodes). There is a total of 9747 DOF. Continuity in mesh points and hence nodes is not enforced at the edges of neighboring elements.

The shaded surfaces ABbFEa and CDdHGc in Figures 3 and 4 are the two likely contact surfaces and the interfaces on the two zones. The engaged length of the splines is 16 mm starting from  $z = 0$  mm (the continuous end) and extending to  $z = 16$  mm (the transition end). Initial gaps of zero magnitudes are imposed on the continuous ends (FE and GH) of the two respective contact surfaces. These initial gaps vary linearly within the engaged length in the axial ( $z$ ) direction of the shaft and achieve a maximum value at the respective transition ends (AB and

CD) of the contact surfaces. The maximum gap value depends on the taper angle being used. The length of the shaft between the transition end and the end of the shaft at  $z = 53$  mm is 37 mm. This length has been chosen in such a way that the edge effects, due to the applied tractions and displacements on the boundary, on the transition end stresses are negligible.

## Results and Discussions

Because the response is non-linear, three different torsional loads, 1490 kN-mm (1100 lb-ft), 2980 kN-mm (2200 lb-in) and 4470 kN-mm (3300 kN-mm), are applied to the shaft. Figures 5 and 6 depict the relationship between the taper angle and the principal and von Mises stress, respectively. Figures 5 and 6 show that as the taper angle increases, the maximum principal or von Mises stress decreases, and after the corresponding stress reached a minimum value, the stress increases if the taper angle further increases. The “optimal” angle at which the minimum stress occurs depends on the applied torque and the stress of interest, i.e. principal or von Mises stress. For example in Figure 6, under a torque of 2980 kN-mm (2200 lb-in), the maximum principal stress is 1960 Mpa for an optimal angle of  $0.54^\circ$ . Under the same torque without taper, the corresponding stress is 2290 Mpa. So the maximum principal stress in the shaft is reduced by 14.4% by tapering the external spline by  $0.54^\circ$ . The minimum von Mises, however, occurs at a taper angle of  $0.09^\circ$ , independent of the applied torque. At this angle, the von Mises stress is reduced by 6%. Our major interest is the fatigue life of the shaft under a design torque of 2980 kN-mm (2200 lb-in). Therefore, unless otherwise stated, subsequent discussions will be devoted to simulation results under this torque.

In this paragraph we next examine the change in the distribution of the contact pressure on the contact surface as a function of the taper angle. The pressures are plotted on the shaded surface ABbFEa along seven lines in the axial direction ( $z$ -direction) as shown in Figures 3 and 4. For example, Line 1 is from F ( $z = 0$  mm) to B ( $z = 16$  mm) and Line 7 is from E ( $z = 0$  mm) to A ( $z = 16$  mm). Intermediate lines are equally spaced between Line 1 and Line 7. The contact pressure profiles in the axial direction for three different taper angles,  $0.0^\circ$ ,  $0.27^\circ$  and  $0.54^\circ$ , are depicted in Figures 7, 8 and 9, respectively. It can be concluded from these three figures that the maximum pressures shift from the transition end BA ( $z = 16$  mm), Figure 3, to the continuous end FE ( $z = 0$  mm) in Figure 4, as the taper angle increases from  $0.0^\circ$  to  $0.54^\circ$ . The pressures are more uniform at an angle of  $0.27^\circ$ . The contact pressure profiles in the transverse direction along the continuous end FE ( $z = 0$  mm) and the transition end BA ( $z = 16$  mm) for three different taper angles are summarized in Figure

10. In this figure, triangles pointing downward and upward represent pressure values in the continuous end and transition end, respectively. This figure shows that the pressures at the continuous end and transition end are very different in magnitude at taper angles of  $0.0^\circ$  and  $0.54^\circ$ . With an angle of  $0.27^\circ$ , the same figure also shows that the pressure distributions at the continuous end are close to those at the transition end.

We next investigate the locations of the maximum principal and von Mises stress contours in the shaft for the different taper angles. The contours of these maximum stresses reveal that their locations are in the “valley” near the transition end of the external spline for all taper angles but their magnitudes decrease as the taper angles increase. A torsional fatigue test [5] also indicates that failure initiates near that end of the spline. Furthermore, the zone of larger stresses gradually spreads toward the continuous end. The change of stress and zone spreading are due to the shift of maximum contact pressures from the transition end to the continuous end. At a taper angle of  $0.0^\circ$ , the maximum contact pressure occurs at the transition end close to the location of the largest maximum principal stress. As the maximum contact pressure shifts toward the continuous end as the taper angles increase, the same pressure will have less influence on the stresses in the transition end because the location of the maximum stress is farther away.

One limitation of the model used in this study lies in the assumption that the initial gaps will not affect the stiffness of the tooth. In reality, as the initial gaps become larger the width of the tooth will be reduced. Since the largest maximum principal stress is in the valley, it is unlikely the stress in that area will be changed significantly due to a change of tooth width. It is prudent, however, to propose to perform future studies to include the effects of a change of stiffness in the tooth on the stress in the valley of the spline.

## Conclusions

The external spline stress on the output shaft can be reduced by tapering the spline in the axial direction. The optimal taper depends on the design torque and the type of stress of interest. Under a design torque of 2980 kN-mm (2200 lb-in), the largest maximum principal stress in the shaft is reduced by as much as 14.4% for an optimal tapering of  $0.54^\circ$ . The predicted location of the largest maximum principal and von Mises stress is always in the valley near the transition end of the spline closer to the applied torque. This is the location of failure as confirmed by a torsional fatigue test in the literature [6]. The zone of more significantly higher stresses tends to spread to the other end, the continuous

end, as the taper angle increases. This zone spreading coincides with the shifting of the maximum contact pressure on the contact surface from the transition end to the continuous end as the taper angle increases. The maximum contact pressure has the most effect on the largest stresses when it is located near the transition end. As the maximum contact pressure moves away from the transition end toward the continuous end, it has less influence on the largest stresses. This is contrary to the conjecture that a uniform contact pressure has to be maintained on the contact surfaces in order to achieve minimum stresses in a shaft.

### **Acknowledgments**

The author would like to thank Donald Dewhirst of the CAE Department and Bill Dowling of Manufacturing Systems Department, FRL for their invaluable suggestions. Special thanks also go to David Sell of Gear Design/Production Engineering Department, ATEO for providing spline geometrical data to the author.

### **References**

1. "Modern Methods of Gear Manufacture", National Broach & Machine Division/Lear Siegler, Inc., Mt Clements, MI, 1972.
2. R. W. Cedoz and M. R. Chaplin, "Design Guide for Involute Splines", SAE, Warrendale, PA, 1994.
3. BEASY User Guide, Computational Mechanics Publications, Southampton, U.K. and Boston, MA., 1995.
4. O. C. Zienkiewicz, "The Finite Element Method in Engineering Science", McGraw-Hill, London and New York, 1971.
5. J. Trevelyan, "Boundary Elements for Engineers, Theory and Applications", Computational Mechanics Publications, Billerica, MA, 1994.
6. P. E. Burke and W. Fisher, "Design and Analysis Procedure for Shafts and Splines", Paper No. 680024, SAE, Warrendale, PA, 1968.

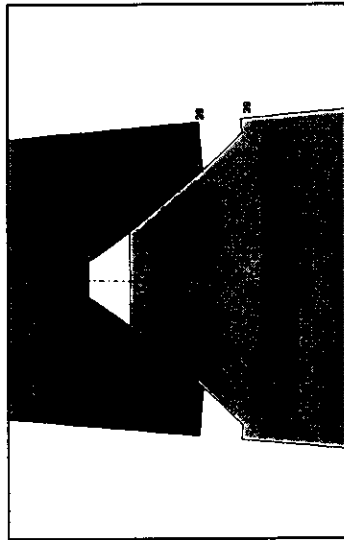


Figure 1: External and internal splines

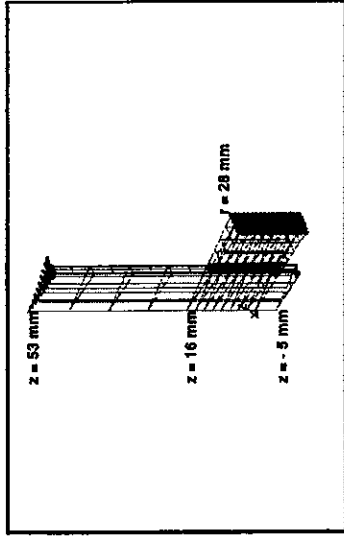


Figure 2: The boundary element

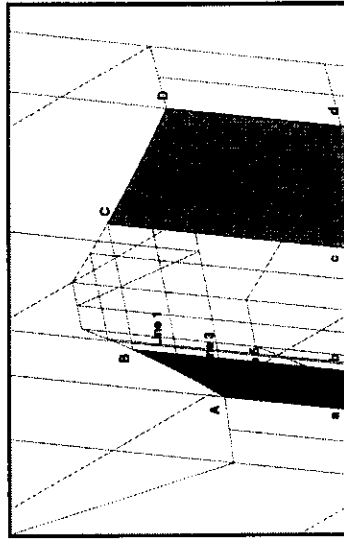


Figure 3: Contact interfaces near transition end in external spline

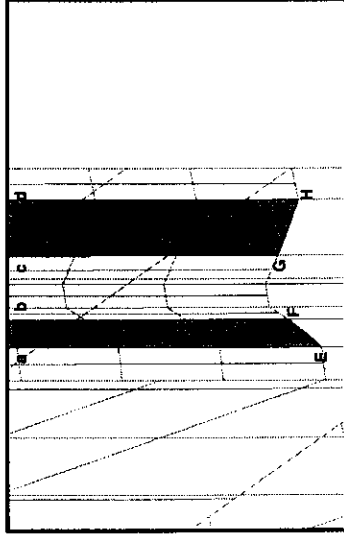


Figure 4: Contact interfaces near continuous end in external spline

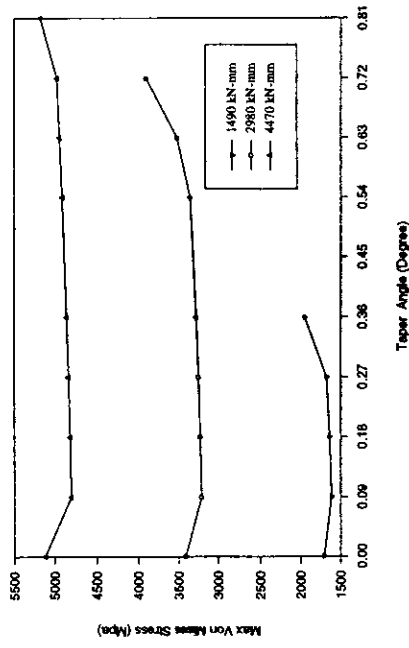


Figure 5: Taper angle vs largest max. principal stress in shaft for different torques

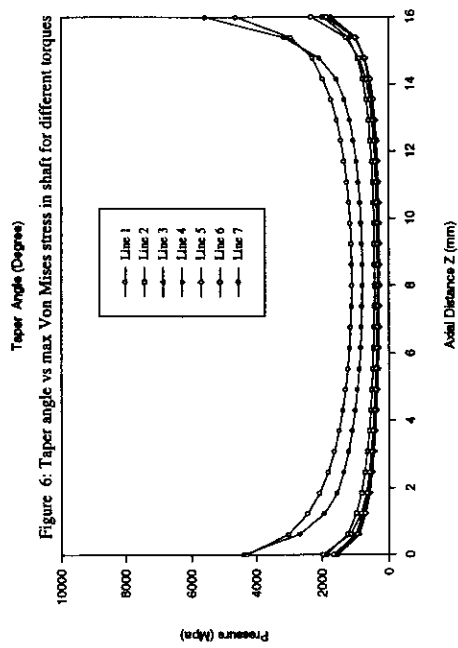


Figure 6: Taper angle vs max Von Mises stress in shaft for different torques

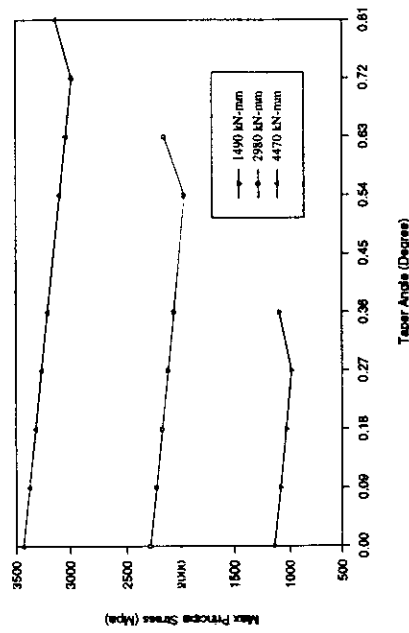


Figure 7: Contact pressure in axial direction for torque = 2980 kN-mm and taper angle = 0.0

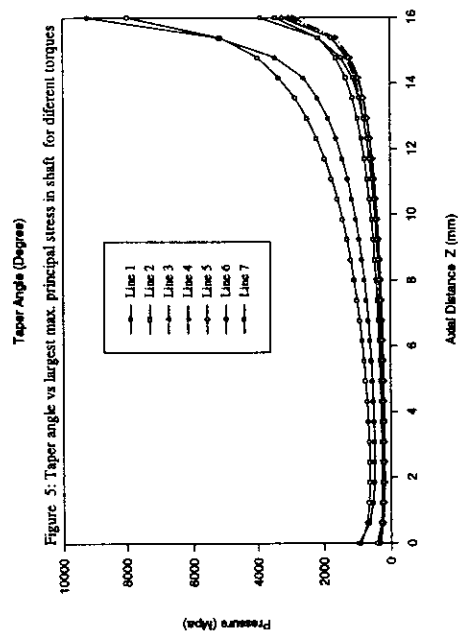


Figure 8: Contact pressure in axial direction for torque = 2980 kN-mm and taper angle = 0.27

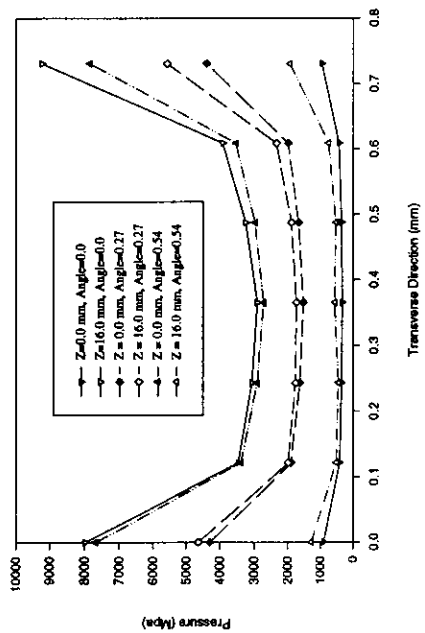


Figure 10: Contact pressure in transverse direction for torque = 2980 kN-mm and different taper angles

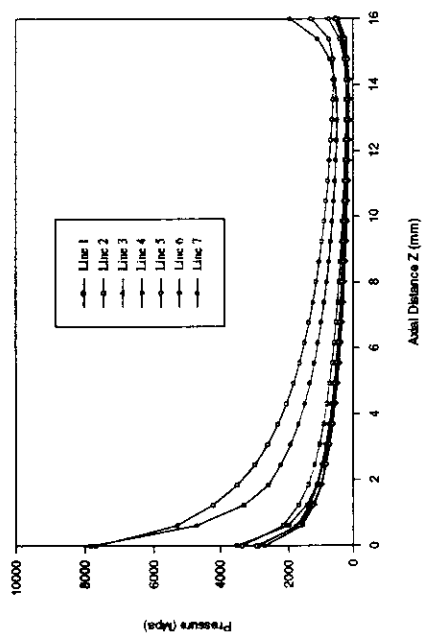


Figure 9: Contact pressure in axial direction for torque = 2980 kN-mm and taper angle = 0.54